CTH-RF-124 February 1997

Investigation of a frequency dependent transfer function and its application to control rod localizaton

by

N. S. Garis and I. Pázsit

CHALMERS UNIVERSITY OF TECHNOLOGY

DEPARTMENT OF REACTOR PHYSICS

ISSN 0281-9775

CTH-RF-124 February 1997

Investigation of a frequency dependent transfer function and its application to control rod localizaton

by

N. S. Garis and I. Pázsit

Department of Reactor Physics
Chalmers University of Technology
S - 412 96 Göteborg, Sweden
ISSN 0281-9775

Investigation of a frequency dependent transfer function and its application to control rod localization

by

N. S. Garis and I. Pázsit

ABSTRACT

Control rod vibrations can be detected via the fluctuations they generate in the neutron flux, i.e. the neutron noise. In a previous paper, a neural network-based algorithm for locating a vibrating control rod from the measured neutron noise was developed. The transfer function used for the core model was based on the so-called power-reactor approximation resulting in a simple, real-valued solution which means that the phase delay of the signal propagation is neglected. In the present work a more realistic transfer function is used, without the approximations present in the previous model. The transfer function is calculated from the Fourier transformed diffusion equation with a complex, frequency dependent buckling, leading to a complex solution. In physical terms, this means that the phase delay of the signal propagation is accounted for. Using such a complex core model, the present paper investigates the effectiveness of applying neural networks for control rod localisation.

1. INTRODUCTION

The detection of vibrations caused by for example control rods via noise measurements is relatively simple, while the localization of which control rod is vibrating is much more complicated. Both the direct task, i.e. calculation of the neutron noise caused by vibrations and the indirect one, i.e. localization of the vibrating control rod by unfolding the neutron noise, are associated with certain difficulties.

Solving the direct task requires mainly the calculation of the Green's function or transfer function of the system. Traditionally, analytical solutions have been preferred. One reason for this was that both the use of the transfer function in the direct task as well as application of the traditional localisation algorithm required analytical manipulations and easy and fast numerical evaluations. In order to get such a simple solution, the core model from which the transfer function was calculated has been kept extremely simple. In all previous work the so-called power reactor approximation was used, which means that the frequency dependent complex buckling was neglected in the defining equation of the transfer function. The result was a real-valued, frequency-independent transfer function in a simple analytical form. Physically, such a function describes the spatial attenuation of the noise in a certain frequency range in reactors of a certain size (actually the range of power reactor sizes and frequencies, hence the name), but does not account for the phase delay of the signal propagation.

The problems of the unfolding stage are only technical, but somewhat lengthier to describe and here we only refer to the discussion in Ref. [1]. One way to overcome the problems concerning the traditional unfolding procedure was to use unfolding methods based on artificial neural networks (ANNs). An ANN-based procedure for the localization of a vibrating control rod was implemented and investigated thoroughly, see Ref. [2]. In this work, just as in the previous ones, the frequency independent transfer function, based on the power reactor approximation, was used. The results have shown that the use of a neural network is an effective and fast method which can be applied on-line.

One advantage of the neural network-based localization technique is however that one is not constrained to use simplified core models. It is therefore a logical step to extend the method by applying a more realistic transfer function. The transfer function of the same 2-D cylindrical reactor model as the one used earlier, but now without the previous approximations, has been recently calculated and investigated. Physically, this means that the phase delay effects in the signal propagation are accounted for. The main purpose of this paper is to report on the performance of the ANN-based localisation technique with this more realistic, complex transfer function. However, the transfer function itself will also be described in some detail because only certain of its properties have been reported so far.

One would expect that since there is more information in the noise signals when phase delay effects are also accounted for, application of the complex transfer function will improve the performance of the localisation technique. This advantage is somewhat offset by the increased complexity of the algorithm which may lead to performance deterioration. Actually, in all reported work so far neural networks use real valued input signals, and there is no prior information available on their performance with complex inputs.

On the reactor physics side, the analysis of the complex transfer function showed that somewhat surprisingly, spatial phase delay effects are very small at plateau frequencies, smaller than at lower frequencies. Thus, there is very little phase delay information availa-

ble at these frequencies. It is not certain that the use of a complex transfer function in combination with a neural network, with its increased network complexity and larger number of nodes will perform better than a simplified (real) transfer function. This question was also investigated in the present report.

2. GENERAL THEORY

One-group neutron diffusion theory with one delayed neutron group is used in a bare, homogeneous cylindrical reactor with extrapolated boundary at core radius R. The vibrations of the control rod are described by a 2-D stochastic trajectory around the equilibrium position $\underline{r}_p$ such that its momentary position will be given by $\underline{r}_p + \underline{\varepsilon}(t)$, where $|\underline{\varepsilon}(t)| \ll R$. According to Feinberg-Galanin theory, the perturbation in the macroscopic absorption cross-section caused by the vibration of the absorber can be written as

$$\delta\Sigma_a(r,t) = \gamma[\delta(\underline{r} - \underline{r}_p - \underline{\varepsilon}(t)) - \delta(\underline{r} - \underline{r}_p)] \tag{1}$$

where γ is Galanin's constant (strength) of the rod.

Using the weak absorber approximation, the neutron noise induced by the vibrating rod can be written in the frequency domain as

$$\delta\phi(\underline{r},\omega) = \frac{\gamma}{D} \cdot \underline{\varepsilon}(\omega) \cdot \nabla_{\underline{r}_p}\{G(\underline{r},\underline{r}_p,\omega) \cdot \phi_0(\underline{r}_p)\} =$$

$$= \frac{\gamma}{D} \cdot \{\varepsilon_x(\omega) G_x(\underline{r},\underline{r}_p,\omega) + \varepsilon_y(\omega) G_y(\underline{r},\underline{r}_p,\omega)\} \tag{2}$$

Here, $\underline{r}$ is the position of the neutron flux detector, $\varepsilon_x(\omega)$ and $\varepsilon_y(\omega)$ are the vibration components in the frequency domain, and G_x and G_y the x and y components of the gradient of the static flux times the Green's function.

The neutron noise given by Eq. (2) is, for small amplitude vibrations, a linear function of the displacement components ε_x and ε_y, whereas it is an implicit function of the rod position $\underline{r}_p$. The determination of the latter, which is much more complicated, can be performed as follows. One selects 3 neutron detectors at positions $\underline{r}_i$, $i = 1, 2, 3$ with measured noise signals $\delta\phi_i(\omega) \equiv \delta\phi(\underline{r}_i, \omega)$. For each detector signal an equation of the form of Eq. (2) is applied. Using two of the equations to eliminate ε_x and ε_y, this results in a symmetric expression where the only unknown parameter is the rod position $\underline{r}_p$ which is given as the root of the equation.

In reality, however, it is not the Fourier transforms of the stationary random processes $\delta\phi_i(t)$ which are used, since the defining integral diverges. Instead, auto- and cross power spectra of $\delta\phi_i(\omega)$ must be used, since they are defined as the Fourier transform of the auto- and cross-correlation functions of the corresponding processes. Likewise, instead of $\varepsilon_x(\omega)$ and $\varepsilon_y(\omega)$, the auto- and cross spectra $S_{xx}(\omega)$, $S_{yy}(\omega)$ and $S_{xy}(\omega)$ of the displacement components need to be used as input source. With application of the Wiener-Khinchin theorem, the auto- and cross spectra of the detector signals can be expressed from Eq. (2) as

$$APSD_{\delta\phi_i}(\omega) = \frac{\gamma^2}{D^2}\{|G_{ix}(\underline{r}_p,\omega)|^2 S_{xx}(\omega) + |G_{iy}(\underline{r}_p,\omega)|^2 S_{yy}(\omega) + 2Re\left[G_{ix}(\underline{r}_p,\omega)\, G_{iy}(\underline{r}_p,\omega)\, S_{xy}(\omega)\right]\} \quad (3)$$

$$CPSD_{\delta\phi_i\delta\phi_j}(\omega) = \frac{\gamma^2}{D^2}\{G_{ix}(\underline{r}_p,\omega)\, G^*_{jx}(\underline{r}_p,\omega)\, S_{xx}(\omega) + G_{iy}(\underline{r}_p,\omega)\, G^*_{jy}(\underline{r}_p,\omega)\, S_{yy}(\omega) + G_{ix}(\underline{r}_p,\omega)\, G^*_{jy}(\underline{r}_p,\omega)\, S_{xy}(\omega) + G_{jx}(\underline{r}_p,\omega)\, G^*_{iy}(\underline{r}_p,\omega)\, S^*_{xy}(\omega)\} \quad (4)$$

As Eqs. (3) and (4) show, calculation of the neutron noise, and thus application of any localisation procedure, requires a model of the displacement component spectra $S_{xx}(\omega)$, $S_{yy}(\omega)$ and $S_{xy}(\omega)$ and the transfer function $G(\underline{r}, \underline{r}_p, \omega)$. The Green's function will be described separately below. Regarding the displacement spectra, simple expressions for these were derived in Ref. [3] from a model of random pressure fluctuations as driving forces of the rod motion. It was found that the possible variety of displacement component spectra can be parametrized by two variables, an ellipticity (anisotropy) parameter $k \in [0, 1]$ and the preferred direction of the vibration $\alpha \in [0, \pi]$ as

$$S_{xx} \propto 1 + k\cos 2\alpha \quad (5)$$

$$S_{yy} \propto 1 - k\cos 2\alpha \quad (6)$$

$$S_{xy} \propto k\sin 2\alpha \quad (7)$$

For an isotropic vibration $k = 0$ while vibration along a straight line has $k = 1$. Between these two extreme values the amplitude distribution of the vibration is an ellipse with the main axis lying in the direction α. As Eq. (7) shows, the cross-spectrum of the displacements, and thus all displacement spectra, are real in this model. The same model will be kept also in the present paper.

3. THE FREQUENCY DEPENDENT TRANSFER FUNCTION

In a homogeneous system, the transfer function $G(\underline{r}, \underline{r}', \omega)$ is defined as the solution of the following Helmholtz-type equation

$$\Delta G(\underline{r}, \underline{r}', \omega) + B^2(\omega)\, G(\underline{r}, \underline{r}', \omega) = \delta(\underline{r} - \underline{r}') \quad (8)$$

where $B^2(\omega)$ is the frequency dependent buckling given by

$$B^2(\omega) = B_0^2\left(1 - \frac{1}{\rho_\infty G_0(\omega)}\right) \quad (9)$$

and $G_0(\omega)$ is the zero-power reactivity transfer function given by

$$G_0(\omega) = \frac{1}{i\omega\left[\Lambda + \frac{\beta}{i\omega + \lambda}\right]} \tag{10}$$

In Eq. (9), B_0^2 is the material buckling and ρ_∞ the infinite reactor reactivity. Since the boundary conditions for the flux or neutron noise are also valid for the Green's function we have

$$G(\underline{r}, \underline{r}', \omega)\big|_{|\underline{r}| = R} = G(\underline{r}, \underline{r}', \omega)\big|_{|\underline{r}'| = R} = 0 \tag{11}$$

Assuming the so-called power-reactor approximation, i.e. $B^2(\omega) \approx 0$, the Helmholtz-type equation in Eq. (8) is converted into a Poisson-type one. The solution of the Green's function can thus be given in a simple closed form, see Refs. [1]-[2]. However, in the present work we keep $B^2(\omega)$ and calculate the solution.

The Green's function of Eq. (8) can be sought in the form

$$G(\underline{r}, \underline{r}', \omega) = G_h(\underline{r}, \underline{r}', \omega) + F \cdot Y_0(B(\omega)|\underline{r} - \underline{r}'|) \tag{12}$$

where G_h is the regular part over the entire core and the term $F \cdot Y_0$ is the irregular one. Since G_h is symmetric, the partial solution can be written as

$$G_h(\underline{r}, \underline{r}', \omega) = \sum_{n=0}^{\infty} A_n J_n(B(\omega) r) \cos(n\varphi) \tag{13}$$

where A_n are constants to be determined from the boundary conditions at $|\underline{r}| = R$, and φ is the angle between $\underline{r}$ and $\underline{r}'$. For the function $Y_0(B(\omega)|\underline{r} - \underline{r}'|)$, we make use of the addition theorem for Bessel functions

$$Y_0(B(\omega)|\underline{r} - \underline{r}'|) = Y_0(B(\omega) r) J_0(B(\omega) r') +$$

$$+ 2 \sum_{n=1}^{\infty} Y_n(B(\omega) r) J_n(B(\omega) r') \cos(n\varphi) \tag{14}$$

The boundary condition at the surface of the reactor determines the constants A_0 and A_n as

$$A_0 = -\frac{F Y_0(B(\omega) R) J_0(B(\omega) r')}{J_0(B(\omega) R)} \tag{15}$$

and

$$A_n = -\frac{2F Y_n(B(\omega) R) J_n(B(\omega) r')}{J_n(B(\omega) R)} \tag{16}$$

Introducing the quantity δ_n defined by

$$\delta_n = \begin{cases} 1, & n = 0 \\ 2, & n > 0 \end{cases} \tag{17}$$

we have

$$G(r, \varphi, r', \varphi' = 0, \omega) =$$

$$\frac{1}{4}\left[Y_0(B(\omega)|\underline{r} - \underline{r}'|) - \sum_{n=0}^{\infty} \frac{\delta_n Y_n(B(\omega)R) J_n(B(\omega)r')}{J_n(B(\omega)R)} J_n(B(\omega)r)\cos(n\varphi) \right] \quad (18)$$

The remaining constant F of (12) was determined by substituting the Bessel function Y_0 with $2\ln[B(\omega)r]/\pi$ for small arguments and then integrating over an area with radius ε around the singularity. Letting $\varepsilon \to 0$, the constant F becomes equal to $1/4$, the factor multiplying the r.h.s. of (18). Since the transfer function of (18) is now complex, then, as Eq. (4) shows, the neutron noise cross-spectra will also be complex, even if the displacement spectra given by Eqs. (5) - (7) are all real.

An analysis of the spatial and frequency dependence of the complex transfer function (18) revealed a somewhat unexpected feature that has not been noticed before. It turned out that the space dependence of the phase delay out from the source point is not a monotonously increasing function of the frequency. This phenomenon is illustrated in Fig. 1. As Fig. 1a shows, at any spatial point the amplitude is a monotonous function of frequency. The space dependence of the transfer function becomes more and more localised around the source with increasing frequencies. The space dependence of the phase shows however a different pattern. At low frequencies the phase slope is small - the phase delay is nearly the same everywhere. With increasing frequencies, the slope starts to increase, but when at the plateau region, in this case within 0.5 - 5 rad/s, it becomes small again (collective response in the whole reactor). Only at even larger frequencies will the slope increase again, showing different phase delays in different parts of the reactor.

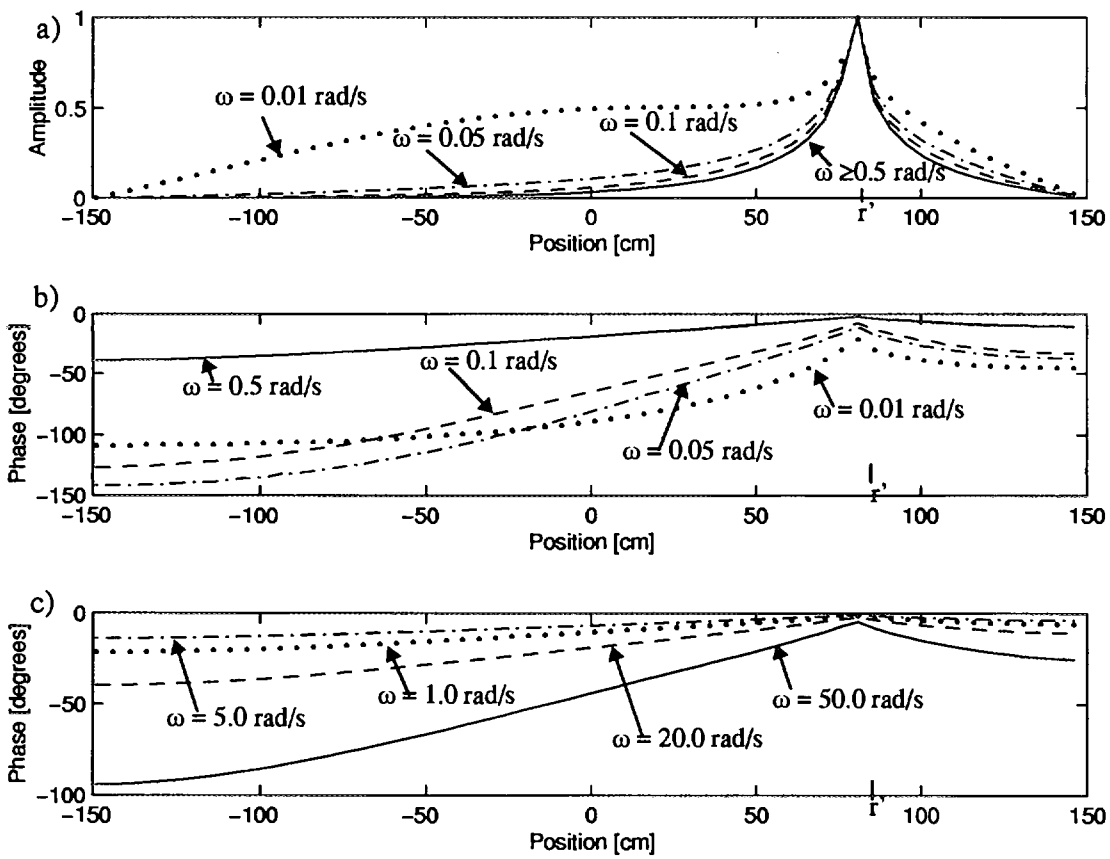

Fig. 1. Space dependence of the amplitude and the phase of the neutron noise in the considered reactor system for several frequencies.

This behaviour was reported and analysed recently in Ref. [4]. It was also mentioned there that this phenomenon amounts to the fact that space-dependent effects are weak at both very low frequencies and at plateau ones. Space-dependent diagnostics, e.g. rod localisation, can be therefore easier at, say, 0.05 rad/s than in the range 0.5 - 5 rad/s. However, the complex frequency dependent transfer function has not been used before for confirming the above statement in a diagnostic task. Since we shall perform rod localisation by using this transfer function, one partial objective of the present paper will be to investigate the performance of the localisation procedure as a function of the frequency.

4. APPLICATION OF NEURAL NETWORKS

The use of neural network (NN) techniques represents a very powerful method for complex problems. Neural networks have been used extensively in the nuclear engineering field for both parameter estimation and diagnostics. Successful applications or pilot studies include diagnostics of steam generators, vibration properties, sensor validation, valves, feedwater flow, estimation of moderator temperature coefficients, BWR stability margins, detection of anomalies, localisation of vibrating control rods and noise spectra analysis. A review of principles and nuclear applications is found in Ref. [5].

One type of neural networks which has become popular is the so called standard three-layered feed-forward network with backward error propagation. The advantages of this type are that it is relatively simple to realize and any continuous function can be modelled if certain conditions are fulfilled. Further details of the structure of the network, the training procedure and other details such as network optimization can be found in Refs. [2] and [5]. A schematic view of the training procedure is shown in Fig. 2 and the structure of the network is shown in Fig. 3. The input nodes consist of the neutron detector auto-spectra and the real and complex parts of the cross-spectra. The number of the nodes depends on the number of detectors used. As in previous work, the cases of 3 and 4 detectors will be investigated. In the first case one has 9 input nodes (3 auto and 2x3 cross-spectra), in the second 16 input nodes (4 auto and 2x6 cross-spectra. The number of output nodes is equal to the number of the control rods. The node corresponding to the vibrating rod is expected to give unity and the rest zero as output. Similarly to previous work, seven output nodes will be taken corresponding to the bank of 7 rods of the VVER type Paks-2 reactor in Hungary in which such a localisation was earlier performed, see Ref. [1].

A performance test, similar to the previous works but with the complex transfer function was performed. Such an investigation consists of training of the network with simulated data (training patterns) and a subsequent test of it by further data in which the success and reliability ratios of the performance of it were investigated. In a general case, such an investigation includes even finding the optimum value of some freely adjustable parameters such as the learning and momentum rates and the number of hidden nodes. However, for the sake of comparison, the same values of these parameters were used as in earlier work. This also means that the network was not specifically optimized for the present investigation.

The results, in compact form, are summarized in Table 1. They will be explained and discussed below. The following facts or properties were investigated:

- a) choice of input data representation;
- b) dependence of the performance on frequency;

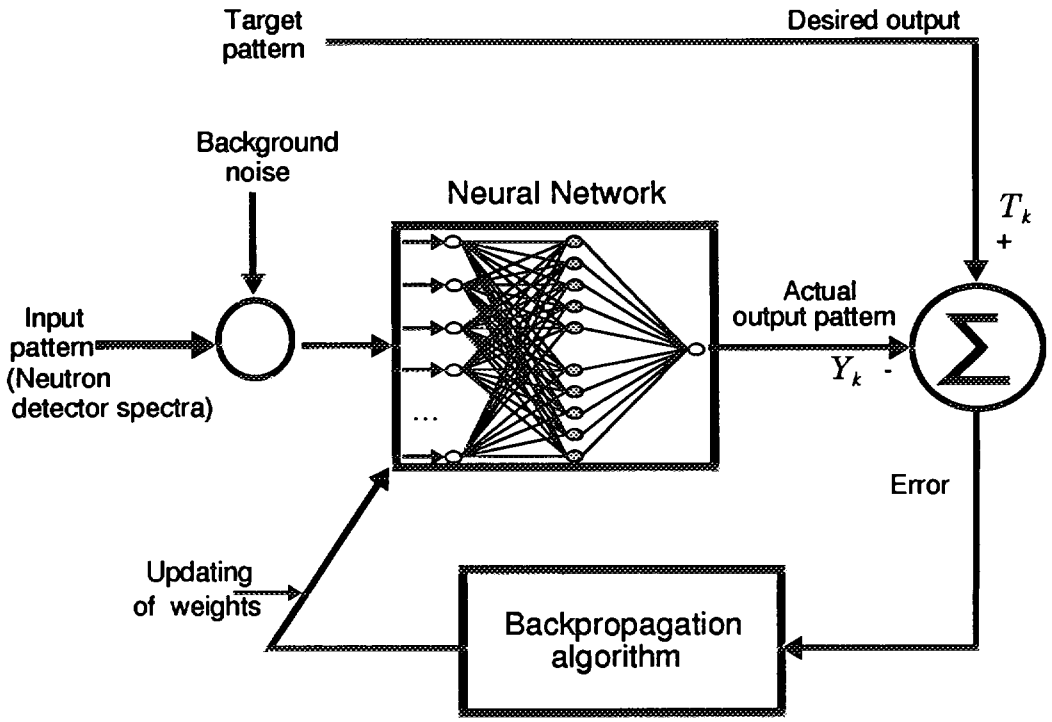

Fig. 2. The training phase of the neural network.

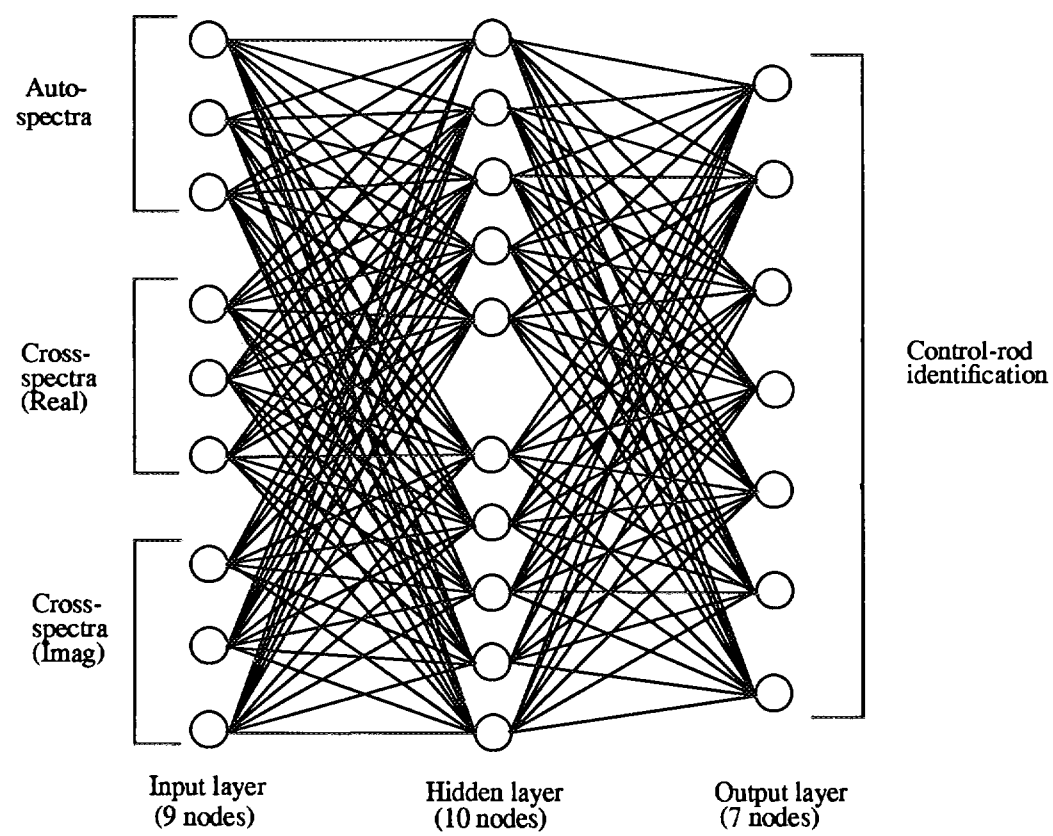

Fig. 3. Structure of the implemented neural network for the case of 3 detectors. For the case of 4 detectors, the input layer consists of 16 nodes instead.

- c) comparison of the complex frequency dependent transfer function with simplified, real transfer functions;
- d) the effects of nesting on the performance;
- e) investigation of the erroneous identifications of the trained network.

In all these investigations, the case of the 3 and 4 detectors will be treated in parallel. It was already seen before that the case of 4 detectors always leads to better results, thus this aspect will not be commented on any more. The two cases are taken here only for illustration.

Table 1. Results of the efficiency of the trained network with 3 and 4 detectors for several frequencies. The number of input pattern pairs used is 10 000 and the user-defined value of the total rms output error is 0.05.

Frequency [rad/s]	3 detectors				4 detectors			
	Training cycles	CPU [s]	Success ratio [%]	Reliability ratio [%]	Training cycles	CPU [s]	Success ratio [%]	Reliability ratio [%]
$B(\omega) \approx 0$	550	570	99.5	**85.3**	41	52	99.2	**96.9**
$G_0(\omega) \approx 1/\beta$	12525	12956	99.7	**92.6**	572	607	99.6	**98.9**
0.005	142	158	99.5	**96.7**	136	228	99.0	**95.2**
0.01	26	34	99.7	**99.1**	48	84	99.1	**95.2**
0.05	62	74	99.8	**98.9**	57	98	99.3	**97.2**
0.10	258	290	99.9	**91.9**	94	158	99.9	**99.1**
0.50	2067	2312	99.8	**85.7**	397	639	99.6	**98.8**
1.0	3262	3681	99.8	**96.2**	435	700	99.6	**98.9**
5.0	3918	4355	99.7	**71.2**	460	750	99.7	**99.1**
20.0	2986	3324	99.6	**89.6**	467	783	99.6	**98.7**
50.0	1285	1402	99.9	**97.9**	405	680	99.9	**99.4**
100.0	4565	5286	99.8	**89.0**	130	222	99.9	**97.9**
200.0	34612	39714	99.6	**97.4**	280	488	99.9	**84.7**

a) Choice of input data representation

Regarding the complex detector cross-spectra, they must be represented by two real numbers each since the weight update of the network (gradient descent method) is defined on real numbers only. One could use either the absolute value and the phase of the CPSDs, or their real and imaginary parts, respectively. Since the amplitude and phase have simple physical interpretations, it was expected that their use would be more effective. Somewhat surprisingly, it turned out that the network input data normalisation was easier and the network was more effective when the real and imaginary parts of the spectra were used instead.

This is not seen in the data of Table 1, which are all based on results by using the real and imaginary parts of the spectra.

b) Dependence of the performance on frequency

The results in Table 1 show the performance of the network for several frequencies. The parameters used for judging the performance is the number of training cycles necessary to attain a pre-defined root mean square (rms) error of 0.05, the success ratio (the ratio of successful identifications in the recall phase compared to the total identifications) and the so-called reliability ratio. The latter concept was developed in Ref. [2] in order to find a confidence parameter of the individual identifications, and can be described briefly as follows. Two parameters were selected, 1) the numerical value of the largest output node, x; 2) the ratio $y = (x - x_{-1})/x$ where x_{-1} is the second largest output node. Out of all points, the ones corresponding to cases of faulty rod identification lie in a restricted area of the (x, y) plane, being concentrated in the lower left hand side of the accessible area. Thus, all identifications (both faulty and correct) within the rectangle denoted, can be classified as "unreliable", and the result is rejected. A confidence parameter called the "reliability ratio" can be obtained by calculating the ratio of the non-rejected identifications to the total number of identifications which is also given in Table 1. It can be seen that unlike the success ratio, the reliability ratio shows a much larger sensitivity on the frequency.

The effect of the non-monotonous dependence of spatial effects on frequency, mentioned in Section 3, can be seen in the results of Table 1. For very low frequencies, a moderate number of training cycles is necessary, but the reliability ratio is not too high. In the range $\omega = 0.01 - 0.05$ rad/s, the space dependent effects become larger, hence the number of training cycles decreases and the reliability ratio increases. Between $\omega = 0.05$ and 20 rad/s, the space effects become weaker again; the number of training cycles increases significantly, and the reliability ratio decreases for the 3-detector case. At even higher frequencies, the space effects are again larger, but at the same time, the magnitude of the noise decreases, thus roughly speaking the network performance remains unchanged on the whole.

c) Comparison with simpler, approximate transfer functions

As mentioned, in earlier work the frequency independent transfer function of the power reactor approximation was used, which is obtained by assuming

$$B^2(\omega) = 0 \tag{19}$$

in Eq. (8). The advantage of this approximation was that a simple real-valued analytical solution could be obtained in the homogeneous reactor used in this study. There is, however, another possibility for an approximate, frequency independent real valued transfer function, which is less restrictive than the power reactor approximation (i.e. can be used with arbitrary reactor size) and more important, with inhomogeneous systems. This is based on the observation of Ref. [4], mentioned also in Section 3, that the phase is almost zero everywhere at plateau frequencies. This fact can be used to set the phase exactly to zero by assuming

$$G_0(\omega) \approx \frac{1}{\bar{\beta}} = \text{const} \tag{20}$$

in Eq. (10), which will lead to the frequency independent real dynamic buckling

$$B^2(\omega) \approx B_0^2\left(1 - \frac{1}{\$_\infty}\right) = \text{const} \qquad (21)$$

where $\$_\infty = \rho_\infty/\beta$. This approximation neglects the phase information just as the power reactor approximation does but describes the space dependence of the noise amplitude better. We will call this the plateau-frequency approximation.

In the present calculations, the plateau-frequency approximation (21) does not lend any numerical advantages, since still the complex solution (18) is used, with $B^2(\omega)$ substituted by (21). The idea here was rather to test the approximation. However, the incentive is that if it works, the approximation can be implemented in static ICFM codes with relatively moderate effort. In principle, one only has to replace $\nu\Sigma_f$ with $\nu\Sigma_f(1-\beta)$, and solve the diffusion equation in the resulting subcritical system with a source. This way the real, frequency independent transfer function at the plateau frequency region can be calculated. This suggestion will be investigated and discussed further in future work.

Concerning the localisation problem, the performance of the power reactor and plateau-frequency approximations can be judged from the first two rows of Table 1. It is seen that the power reactor approximation performs comparably with or is somewhat worse than the full solution at plateau frequencies. However, the plateau-frequency approximation is fully comparable with the full solution at these frequencies in the case of 4 detectors and it is better than the full solution in the case of 3 detectors. By better we mean the larger reliability ratio. The number of training cycles required is larger for the approximative model, but this is only a slight disadvantage, because the training is done off-line, and also, calculating the training patterns is faster in a simple transfer function model.

In summarizing, the plateau-frequency approximation appears to be a promising candidate for calculating the transfer function for plateau frequencies with e.g. nodal methods. It is thus also seen that the approximation (20), used formerly in point kinetic models, can also be extended to space-dependent calculations.

d) The effects of nesting on the performance

In all the cases reported so far, whether 3 or 4 detectors, the detector positioning on the (r, φ) plane was such that the radial distance from the core centre, r_d, was the same for all detectors, the angular spacing φ of the detectors uniform, and all control rods were inside the circle spanned by r_d ("nesting"). In reality, such an arrangement may not always be possible to achieve due to technical constraints. Besides, it is not granted either that the symmetric arrangement is the optimum one. Thus it is interesting to investigate the performance of other detector geometries as well.

Some results of such an investigation are shown in Table 2 where the angular spacing of the detectors is kept uniform while the radial distance is varied. It is seen that by increasing the radial distance of the detectors, i.e. increasing nesting of the control rods, the number of training cycles to attain a given rms output error is decreasing. However, due to the infinity of possible asymmetric arrangements, and the large number of possible parameters to take into account, a concise quantitative summary of the results is impossible. Here we confine ourselves to note the general trend that with increasing unevenness of angular detector spacing, and decreasing nesting, the number of training cycles to attain a given rms output error will rise increasingly.

Table 2. Results of the efficiency of the trained network for different detector positions using the vibration frequency of 1.0 rad/s. The angular spacing of the detectors is uniform while the radial distance is varied.

Position of the 1st detector (x,y) [cm]	4 detectors		
	Training cycles	Success ratio [%]	Reliability ratio [%]
(100, 0)	1405	99.2	97.8
(110, 0)	771	99.5	98.8
(120, 0)	435	99.6	99.0
(130, 0)	303	99.5	98.5
(140, 0)	263	99.5	98.1
(100, 10)	506	99.8	98.9
(110, 10)	181	99.7	99.0
(120, 10)	164	99.6	98.8
(130, 10)	140	99.5	99.2
(140, 10)	118	99.4	98.9
(100, 20)	1187	99.6	96.3
(110, 20)	579	99.5	98.0
(120, 20)	224	99.2	97.4
(130, 20)	156	99.1	98.2
(140, 20)	144	99.1	97.5

e) Investigation of the erroneous identifications of the trained network

In an earlier paper, see Ref. [2], it was suggested that one way to improve the efficiency of the neural network would be to check whether the faulty identifications are related to certain and unusual values of anisotropy (k) and preferred direction of the vibration (α) or not. In Fig. 4, the distribution of faulty identifications is shown w.r.t. control rods, k and α for the first three cases in Table 1. It can be seen that the faulty identifications for all three cases are related to both certain control rods and directions. Another interesting result is that faulty identifications occur for only very high k-values. Since the cases with high k-values correspond to extreme anisotropy which are unlikely to occur in reality, this means that the efficiency of the network can be improved by just neglecting these extreme values in both the training and the identification.

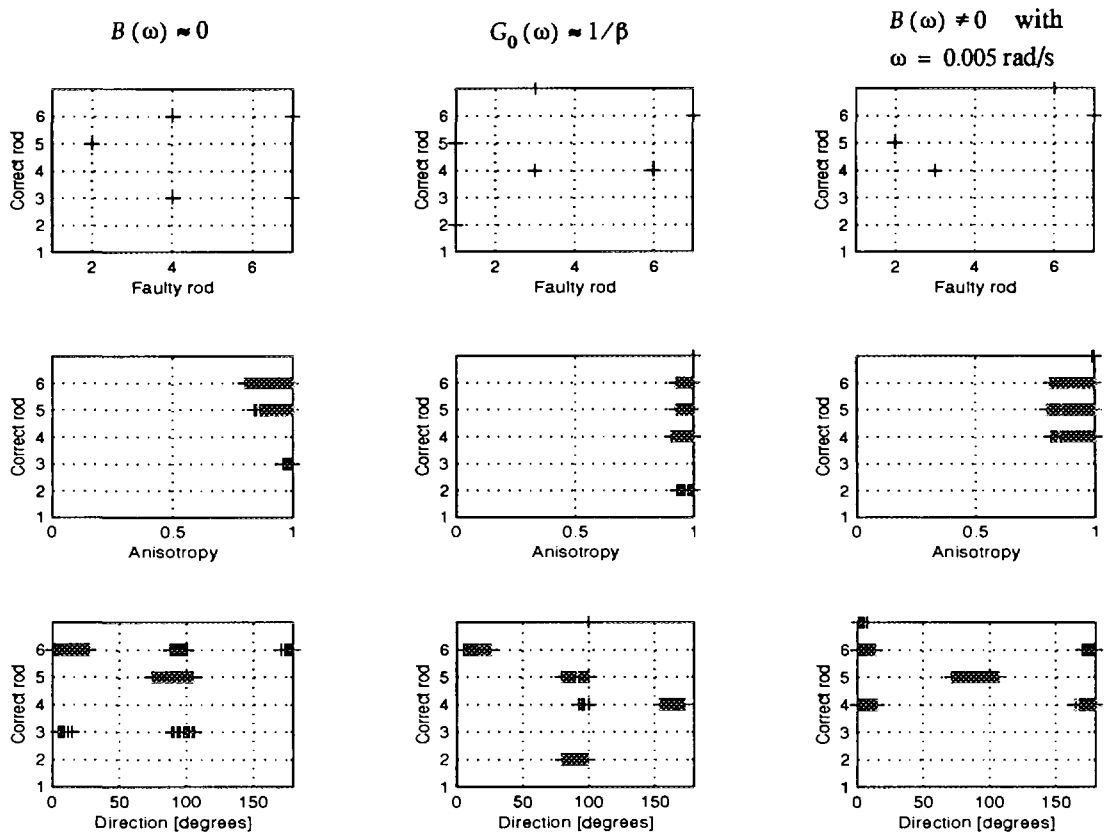

Fig. 4. The distribution of faulty identifications w.r.t. control rods, anisotropy (ellipticity) and preferred direction of the vibration for the first three cases in Table 1.

5. CONCLUSIONS AND FUTURE WORK

The above results show that the use of a neural network for control rod localisation is an effective method. In particular, a neural network provides an easy-to-use method with an explicit result (gives the suspected rod position directly) and the classification procedure is very fast, thus the method can be applied on-line. The reliability ratio is very close to the industrial standard of 0.1% accepted false or missed alarm rate in monitoring and surveillance systems. The numerical simulations have also shown that the localisation task becomes difficult for vibrations within the plateau region. The recommendation of using four detectors instead of three is still valid.

We have so far been concerned with the monitoring of the whole core, i.e. with all rods. Another strategy could be to concentrate on certain rods at a time, confined e.g. in one quadrant of the core, and select symmetrical detector geometries with nesting with respect to the rods selected. Such a possibility exists in Westinghouse type reactors such as the Ringhals 2 - 4 units in Sweden, where there are no fixed in-core detectors available, but 4 movable detectors can be inserted at a time into various positions. Then, different combinations of 4 detector positions can be selected to monitor various parts of the core, or selected rods/fuel bundles.

So far no attention has been paid to the determination of vibrating properties in connection with the neural-based localization technique. In earlier papers dealing with the traditional localization technique, see e.g. Ref. [1], it has been shown that once the rod position

is known, the vibration spectra can be explicitly expressed by the transfer function and the neutron noise spectra. An alternative would be to include k and α of Eqs. (5), (6) and (7) directly into the network structure and use it both in the training and the identification. If the faulty identifications are still related to e.g. extreme anisotropy values, then the extreme anisotropy values produced by the network could be classified as "unreliable" which in turn would provide the identification with an additional confidence parameter. This surmise will be investigated in later work.

In the present paper, we have shown that for the NN based localisation technique a more complex transfer function does not constitute a difficulty. This means that one is not constrained to use simplified core models. The investigations of course do not have to be confined to model based transfer functions. The final goal is to use methods in which the transfer function of a realistic core can be calculated, such as in Refs. [6] and [7].

ACKNOWLEDGEMENTS

This work was supported by a research grant from the Swedish Nuclear Power Inspectorate, Grant No. R14.5 960691 - 96096.

REFERENCES

[1] I. Pázsit and O. Glöckler, "On the Neutron Noise Diagnostics of BWR Control Vibrations-III. Application at a Power Plant." *Nucl. Sci. Engng.* **99**, 313(1988).

[2] I. Pázsit, N. S. Garis and O. Glöckler, "On the Neutron Noise Diagnostics of Pressurized Water Reactor Control Vibrations-IV: Application of Neural Networks." *Nucl. Sci. Engng.* **124**, 167(1996).

[3] I. Pázsit and O. Glöckler, "On the Neutron Noise Diagnostics of Pressurized Water Reactor Control Vibrations-II. Stochastic Vibrations." *Nucl. Sci. Engng.* **88**, 77(1984).

[4] N. S. Garis and I. Pázsit, "On the Kinetic Response of a Reactor with Delayed Neutrons II: Spatial Effects". *Ann. Nucl. En.*, **23**, 1143 (1996).

[5] I. Pázsit and M. Kitamura, (1996) "The Role of Neural Networks in Reactor Diagnostics and Control". To appear in *Advances in Nuclear Science and Technology*, Vol. 24.

[6] M. Makai, "Nodewise Analytical Calculation of the Transfer Function". *Ann. Nucl. En.*, **21**, 519 (1994).

[7] F. Hollstein and K. Meyer, "Calculation of Neutron Noise Due to Control Rod Vibration Using Nodal Methods for Hexagonal-Z-Geometry". Seventh Symposium on Nuclear Reactor Surveillance and Diagnostics, SMORN-VII, Avignon, France, June 19-23, 1995.